

# Exploring the use of soft X-ray microscopy for imaging subcellular structures of the inner ear<sup>1</sup>

GÖRAN A. JOHANSSON\*, SHYAM M. KHANNA†, AJIT NAIR‡, PAULA MANNSTRÖM§, GREG DENBEAUX‡ & MATS ULFENDAHL§

\*Biomedical and X-ray Physics, Department of Physics, Royal Institute of Technology, SE-106 91 Stockholm, Sweden

†Department of Otolaryngology/Head and Neck Surgery, Columbia University, New York, NY 10032, U.S.A.

‡Center for X-ray Optics, Lawrence Berkeley Laboratory, University of California, Berkeley, CA 94720, U.S.A.

§Center for Hearing and Communication Research, and Department of Clinical Neuroscience, Karolinska Institutet, Karolinska University Hospital, SE-171 76 Stockholm, Sweden

**Key words.** Hair cell, inner ear, Reissner's membrane, soft X-ray microscopy, tectorial membrane.

## Summary

The soft X-ray microscope at the Lawrence Berkeley National Laboratory was developed for visualization of biological tissue. Soft X-ray microscopy provides high-resolution visualization of hydrated, non-embedded and non-sectioned cells and is thus potentially an alternative to transmission electron microscopy. Here we show for the first time soft X-ray micrographs of structures isolated from the guinea-pig inner ear. Sensory outer hair cells and supporting pillar cells are readily visualized. In the hair cells, individual stereocilia can easily be identified within the apical hair bundle. The underlying cuticular plate is, however, too densely composed or too thick to be clearly visualized, and thus appears very dark. The cytoplasmic structures protruding from the cuticular plates as well as the fibrillar material surrounding and projecting from the cell nuclei can be seen. In the pillar cells the images reveal individual microtubule bundles. Soft X-ray images of the acellular tectorial membrane and thin two-layered Reissner's membrane display a level of resolution comparable to low-power electron microscopy.

## Introduction

To investigate the true structural and functional properties of cells, it is essential to study them under as intact and

physiological conditions as possible. Each experimental method, however, reflects a combination of advantages and disadvantages. For example, light microscopy allows studying living cells but with a limited spatial resolution. In addition, for high spatial resolution imaging of thin objects, the contrast for biological samples is quite poor and contrast enhancement techniques, e.g. fluorophore staining and phase contrast microscopy, are frequently used. Transmission electron microscopy, by contrast, offers much greater spatial resolution but is primarily used for fixed, dehydrated, embedded and, finally, sectioned tissue. In addition, the processing efforts required prior to visualization are laborious and time consuming. Clearly, a microscope technique combining the advantages of light and electron microscopes would be very powerful.

The soft X-ray microscope offers a highly interesting method for imaging intact hydrated cells, with high natural absorption contrast and with a spatial resolution beyond what is achievable with visible light microscopy (Schmahl *et al.*, 1993; Kirz *et al.*, 1995; Meyer-Ilse *et al.*, 1995; see also review by Yamamoto & Shinohara, 2002). The reason is that in the soft X-ray region the interaction between matter and electromagnetic radiation is particularly strong and highly wavelength dependent (Attwood, 1999). By a slight change in wavelength, the photon absorption can change by several orders of magnitude and, for a selected wavelength, one material can be almost transparent and another material highly absorbent. Its resolution falls between that of light microscopy and high-resolution electron microscopy, and is presently limited by the available diffractive X-ray optics to 20 nm. Exposure times in the soft X-ray microscope are usually a few seconds, which creates the potential for making several hundred images per day. Furthermore,

Correspondence to: Dr Mats Ulfendahl. Tel.: +46 851776307; fax: +46 8301876; e-mail: mats.ulfendahl@cfn.ki.se

<sup>1</sup>This paper is dedicated to the memory of Dr Werner Meyer-Ilse. Werner was the key moving force in the design and fabrication of the X-ray microscope XM-1 at ALS. He inspired us to work on the application of X-ray microscopy to the inner ear and helped us with his encouragement and support.

sample handling is as easy as in visible light microscopy and it can utilize non-dehydrated and non-embedded tissue immersed in buffer solutions without any contrast enhancement techniques.

The soft X-ray microscope at the Lawrence Berkeley National Laboratory has been developed for the visualization of biological specimens (Denbeaux *et al.*, 2001; Meyer-Ilse *et al.*, 2001). In the present report, we explore, for the first time, the use of soft X-ray microscopy to examine elements from the guinea-pig inner ear. The main aim of the study was to compare the visualization of different cellular elements using transmission electron microscopy and soft X-ray microscopy, especially regarding the relative efficiency of the two techniques in terms of the information they provide with respect to the preparation time needed.

## Materials and methods

### Cell and tissue preparations

Cells were isolated from the hearing organs of albino guinea-pigs (female, 250–300 g,  $n = 8$ ; Simonsen Laboratories, Inc., Gilroy, CA, U.S.A.). The animals were deeply anaesthetized using carbon dioxide and rapidly decapitated. The temporal bones were excised and stored on ice until they were transferred to tissue culture medium (minimum essential medium with Hanks' salts; Life Technologies/GibcoBRL), where the middle ear cavity was opened to expose the cochlea. The bony shell of the cochlea as well as the stria vascularis were removed, and the coils of the hearing organ were gently scraped off the basilar membrane using a fine-tipped scalpel. Following brief enzymatic digestion (collagenase type I, 0.5 mg mL<sup>-1</sup>, 3 min; Sigma Chemical Co.) and repeated rinsing, the cells are dispersed using gentle mechanical treatment. The isolation

procedure has been developed to produce individual outer hair cells but also other cell types can be found, e.g. supporting cells such as pillar cells (see Fig. 1). The isolated cells were immediately fixed using 3% glutaraldehyde in phosphate buffer (0.1 M, pH 7.3) and stored in Eppendorf tubes at room temperature. To enhance the number of cells for visualization, the solutions were left to settle and only the 'pellets' were used. In some experiments the tubes were centrifuged to further increase the density of the cells. In a separate series of experiments (using pigmented guinea-pigs) tissue samples were prepared from the Reissner's membrane and tectorial membrane. The cochlea was exposed and the tissue fixed *in situ* using 2.5% glutaraldehyde in tissue culture medium (minimum essential medium with Hanks' salts; Life Technologies/GibcoBRL). Using fine scalpels and forceps, parts of the membranes were microdissected and stored in fixative. A small drop (10–20 µL) of the cell or tissue suspension (containing also the fixative) was then transferred to the so-called wet cell (#20), which is used in this experiment to keep the biological cells in an aqueous environment during exposure in the soft X-ray microscope. The chamber consists of two circular stainless steel plates, each with a 100-nm-thick silicon nitride membrane glued in its centre. A drop of cell suspension was placed on one of the membranes and the other was placed on top. By slowly pressing the steel plates together the gap between the membranes is decreased until it is comparable with the diameter (~10 µm) of the cells. The wet cell was then placed in a regular light microscope (Zeiss Axioplan) to localize the cells of interest. The coordinates were stored and used to find exactly the same cells using the soft X-ray microscope. The experiments were performed at two sessions, the first aiming at observing thin membranous structures from the inner ear and the second focused on cells isolated from the hearing organ (organ of Corti; Fig. 1).

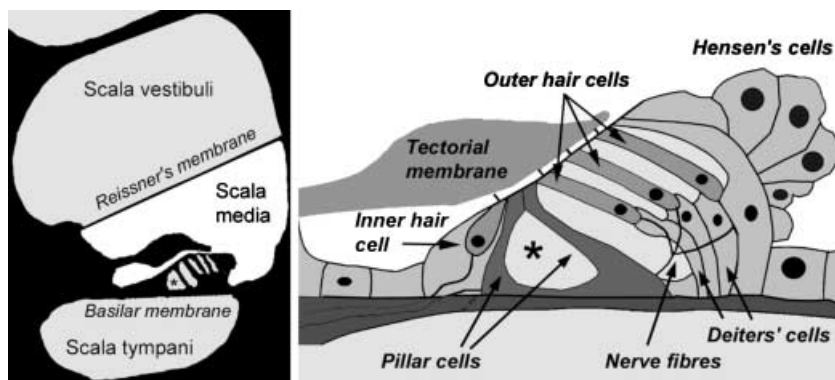


**Fig. 1.** (A) Schematic illustration of one of the turns of cochlea in the guinea-pig inner ear. The cochlea is divided into three fluid-filled compartments. Scala media, containing the hearing organ (organ of Corti), is separated from scala vestibuli and scala tympani by the thin Reissner's membrane and the basilar membrane, respectively. Asterisk, the tunnel of Corti inside the hearing organ. (B) The hearing organ consists of two types of sensory cells, inner and outer hair cells, and several types supporting cells, e.g. pillar cells, Deiters' cells and Hensen's cells. The hair bundles (stereocilia) of the sensory hair cells protrude from the surface of the hearing organ towards the overlying tectorial membrane. The basal ends of the outer hair cells, supported by the Deiters' cells, receive predominantly efferent innervation via nerve fibres projecting from the centre of the cochlea. Asterisk, tunnel of Corti.

The protocol (#18101) for the care and use of animals was approved by the Animal Welfare and Research Committee at the Lawrence Berkeley National Laboratory.

#### *Soft X-ray microscopy*

The soft X-ray transmission microscope (XM-1) (Meyer-Ilse *et al.*, 1995, 1999) located at the Lawrence Berkeley National Laboratory was used to collect the images presented here. The advanced light source (ALS) provides the short-wavelength synchrotron radiation needed for the experiments. In the microscope a condenser zone plate lens focuses the intense soft X-ray beam coming from one of the bending magnets inside the synchrotron onto the sample (Anderson *et al.*, 2000). A pinhole (17  $\mu\text{m}$ ) in front of the sample in combination with the inherently strongly chromatic condenser zone plate lens acts as a monochromator and gives a spectral resolution of  $\lambda/\Delta\lambda > 500$  for the photons reaching the sample. By varying the distance between the condenser zone plate and the pinhole, different wavelengths between 1.4 and 4.1 nm can be selected. The wavelength used in this study was 2.4 nm, which is just above the oxygen K-shell absorption edge ( $\lambda = 2.3$  nm). However, the photon absorption by carbon atoms is high at this wavelength and this ensures that maximum contrast is achieved for biological samples. The soft X-rays can penetrate up to 10- $\mu\text{m}$ -thick samples, which is usually not possible with other types of microscopy methods with similar or better resolution, cf. conventional electron microscopy.

The actual imaging of the sample is performed with a micro zone plate with a focal length of 1100  $\mu\text{m}$  (Anderson *et al.*, 2000) and the magnification used for this experiment was 1950 $\times$ . A peltier-cooled, back-illuminated CCD camera with 1024  $\times$  1024 pixels was used to record the images. In soft X-ray microscopy using diffractive optics the achievable resolution is, generally, limited by the outermost zone width of the zone plate. In this experiment the outermost zone width was 40 nm and the same value is expected for the spatial resolution, although the effective pixel size in the sample plane is 12 nm. Nonetheless, this is an order of magnitude better than with visible light microscopy. The exposure time is typically a few seconds to achieve low-noise images. The field of view for the magnification used is 10  $\mu\text{m}$  in diameter, which is usually too small to allow an image of a complete cell. This limitation can, however, be overcome by acquiring multiple exposures of different parts of the same cell and then using a computer program that automatically combines the images into a single image with a field of view large enough to cover the entire cell. Alignment of the individual images in the composite was possible because the XM-1 control program records the spatial coordinates of every image taken. The computer uses these coordinates to assemble the composites on a grid. The precision alignment of this composite at near the resolution of the microscope was achieved using an auto-correlation routine to position adjacent images (Loo *et al.*, 2000).

#### *Electron microscopy*

For comparison, the hearing organ and Reissner's membrane were prepared for electron microscopy. The animals were deeply anaesthetized with pentobarbiturate (i.p.) and rapidly decapitated. The cochlea was removed and fixed in 3% glutaraldehyde in 0.1 M phosphate buffer at pH 7.4. Following postfixation in 1% osmium tetroxide in 0.1 M phosphate buffer for 1 h, the tissue was dehydrated in ascending concentrations of ethanol, and embedded in plastic resin (Agar 100; Agar Scientific Ltd, Stansted, U.K.). Ultrathin sections were cut on an LKB ultratome. The sections were stained with uranyl acetate and lead citrate and examined in an electron microscope. The time from death of the animal to obtaining an electron microscope image was about 9 days. This included the time for the embedding material to harden etc. The actual technician time used was approximately four full working days.

#### **Results**

The sensory hair cells from the hearing organ are ideal for using with the soft X-ray microscope as their diameter is less than 10  $\mu\text{m}$  (Fig. 2) and they thus precisely fit the experimental chamber. The stereocilia bundles and even individual stereocilia were clearly seen at the apical poles of the outer hair cells (Fig. 3). By contrast, very little of the internal structure of the carbon-dense cuticular plates was revealed. Extending downwards from the cuticular plate a protrusion of dense material could be seen. This infracuticular network is seen only in the long outer hair cells from the apical regions of the cochlea. It has been shown to consist of filamentous actin (Zenner, 1986; Thorne *et al.*, 1987) and to be closely related to microtubules (Steyger *et al.*, 1989; Slepecky & Ulfendahl, 1992). Around and seemingly radiating from the outer hair cell nuclei close to the basolateral cell membrane, abundant filamentous structures were seen (Fig. 4). These structures most likely represent the cytoplasmic intermediate filaments that link the nucleus to the cell membrane and that are suggested to be involved in the organization of the cytoplasm and possibly nuclear transports (see review by Djabali, 1999). Several nerve endings were still attached to the synaptic end of the cells following the isolation procedure (Fig. 4B).

At the present magnification, soft X-ray microscopy provides a field of view of only 10  $\mu\text{m}$  in diameter. This was, however, enough to capture images across the width of the outer hair cells. In order to acquire an image of the entire outer hair cell, several 10- $\mu\text{m}$  images needed to be captured and subsequently (i.e. off-line) tiled. This is illustrated in Fig. 5, which shows a long and slender outer hair cell. During normal image acquisition there are usually no obvious signs of tissue damage. However, during tiling, i.e. when a larger area of the tissue is covered by repeated exposures, radiation damage is apparent (see Fig. 5). Damage is usually expressed as cell shrinkage and, in more severe cases, as disintegration of the plasma membranes.

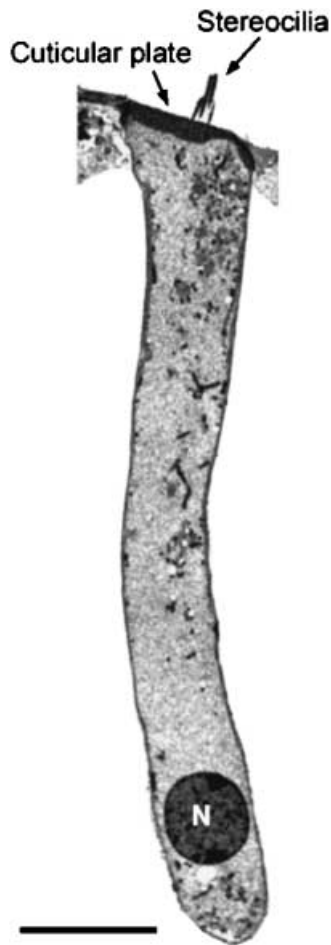


**Fig. 2.** Electron micrograph showing an outer hair cell from the apical regions of the hearing organ. N, nucleus. Scale bar, 10  $\mu\text{m}$ .

To limit potential cell damage in the sample during the focusing procedure, this was performed with a higher binning of the CCD camera and using very short exposure times.

The preparations contained not only outer hair cells but also a small number of supporting cells, mainly pillar cells (cf. Fig. 1B). These cells form the tunnel of Corti and are

thought to provide mechanical stability to the hearing organ. The pillar cells thus have a distinct cytoskeleton containing both large bundles of cross-linked microtubules and plentiful actin filaments (e.g. Kikuchi *et al.*, 1991; Slepecky & Ulfendahl, 1992). Compared with the cell membranes, filamentous structures proved to be more resistant and showed no detectable signs of damage. In the pillar cells, filaments and microtubules were clearly visualized (Fig. 6).

As with the outer hair cells, the thin Reissner's membrane is easily fitted into the chamber. This membrane, consisting of two cell layers but only around 5  $\mu\text{m}$  thick, separates two fluid-filled compartments in the inner ear, scala vestibuli and scala media (see Slepecky, 1996, for an overview and references). The soft X-ray microscope images clearly revealed the structure of the Reissner's membrane (Fig. 7). The membrane consists of two layers. The two cells with dark nuclei (top left and bottom middle) are mesothelial cells that face scala vestibuli whereas the remaining cells with lighter nuclei are epithelial cells facing scala media and the hearing organ (cf. Fig. 1). Cell boundaries and intercellular junctions can be readily identified. The desmosomes (thickening at the middle of an intercellular bridge) seen in the image are between 0.1 and 0.2  $\mu\text{m}$  wide. Inside the cells, nuclei and some mitochondria are clearly defined. There is a fibrous matrix between the cell wall and the nucleus. The matrix may be visible due to the greater depth of focus of the X-ray microscope. For comparison, a transmission electron micrograph of the Reissner's membrane is shown in Fig. 8. This image is similar to that obtained by the X-ray microscope. Mitochondria are better defined and can be seen in greater number. Cell boundaries are sharper and show more detail. However, it is evident that even though the membrane is visualized intact (i.e. not sectioned) and no staining was used, the X-ray microscope image provides structural information comparable with what is seen with electron microscopy, at least at a low magnification.

Compared with the other structures shown here, the tectorial membrane is a more difficult structure to visualize. The membrane, an acellular structure covering the surface of the organ of Corti (see Slepecky, 1996), is quite thick in its natural environment. Although it shrinks significantly during tissue

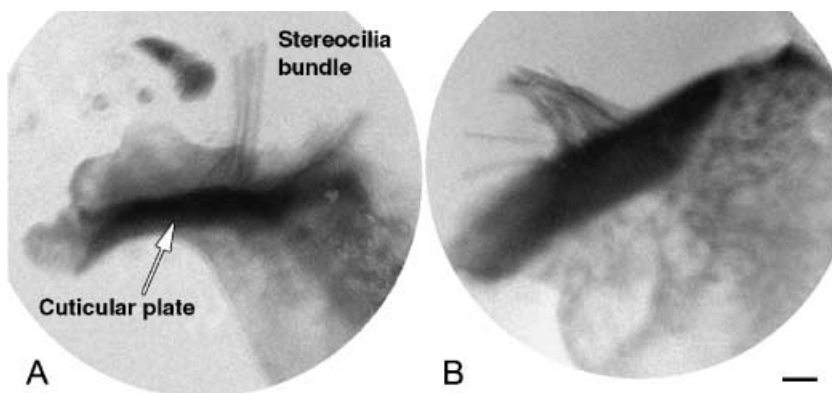


**Fig. 3.** Soft X-ray micrographs showing the apical poles of two outer hair cells. Individual stereocilia can be seen projecting from the dense cuticular plates. Scale bar, 1  $\mu\text{m}$ .

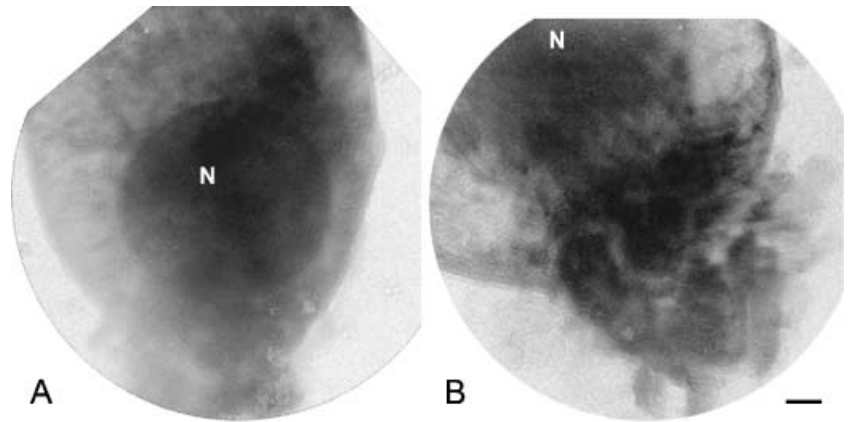


Fig. 4. Soft X-ray micrographs of the basal ends of two outer hair cells. Fibrillar structures are seen surrounding the dense nuclei (N). Scale bar, 1  $\mu\text{m}$ .



Fig. 5. One outer hair cell imaged by tiling 32 individually acquired soft X-ray micrographs. Scale bar, 5  $\mu\text{m}$ .

preparation, only its thinner peripheral regions will fit the chamber of the X-ray microscope. The soft X-ray microscope images revealed its distinctive fibrillar organization (Fig. 9). It has previously been shown using transmission electron microscopy that type A collagen parallel fibrils run in the longitudinal direction, embedded in a matrix of type B fibrils that are branched and coiled (Kronester-Frei, 1978; Tsuprun & Santi, 1996). The diameter of the type A fibrils in the guinea-pig tectorial membrane has been determined to be 10 nm (Kronester-Frei, 1978). Visualization of these fibres in electron microscopy requires special fixation and staining of the tissue (Tsuprun & Santi, 1997) that were not necessary here.

#### Discussion

Transmission electron microscopy, with resolution in the range of 1 nm, is currently the main tool for visualization of subcellular structures. A major disadvantage of electron microscopy is that it can only be applied to fixed, dehydrated and sectioned material. Moreover, the time required for preparing tissue samples for electron microscopy is long and quite laborious. An interesting alternative is offered by X-ray

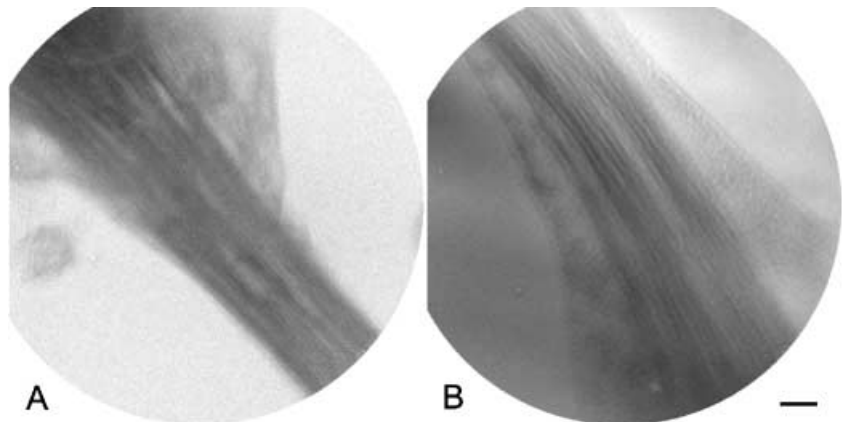
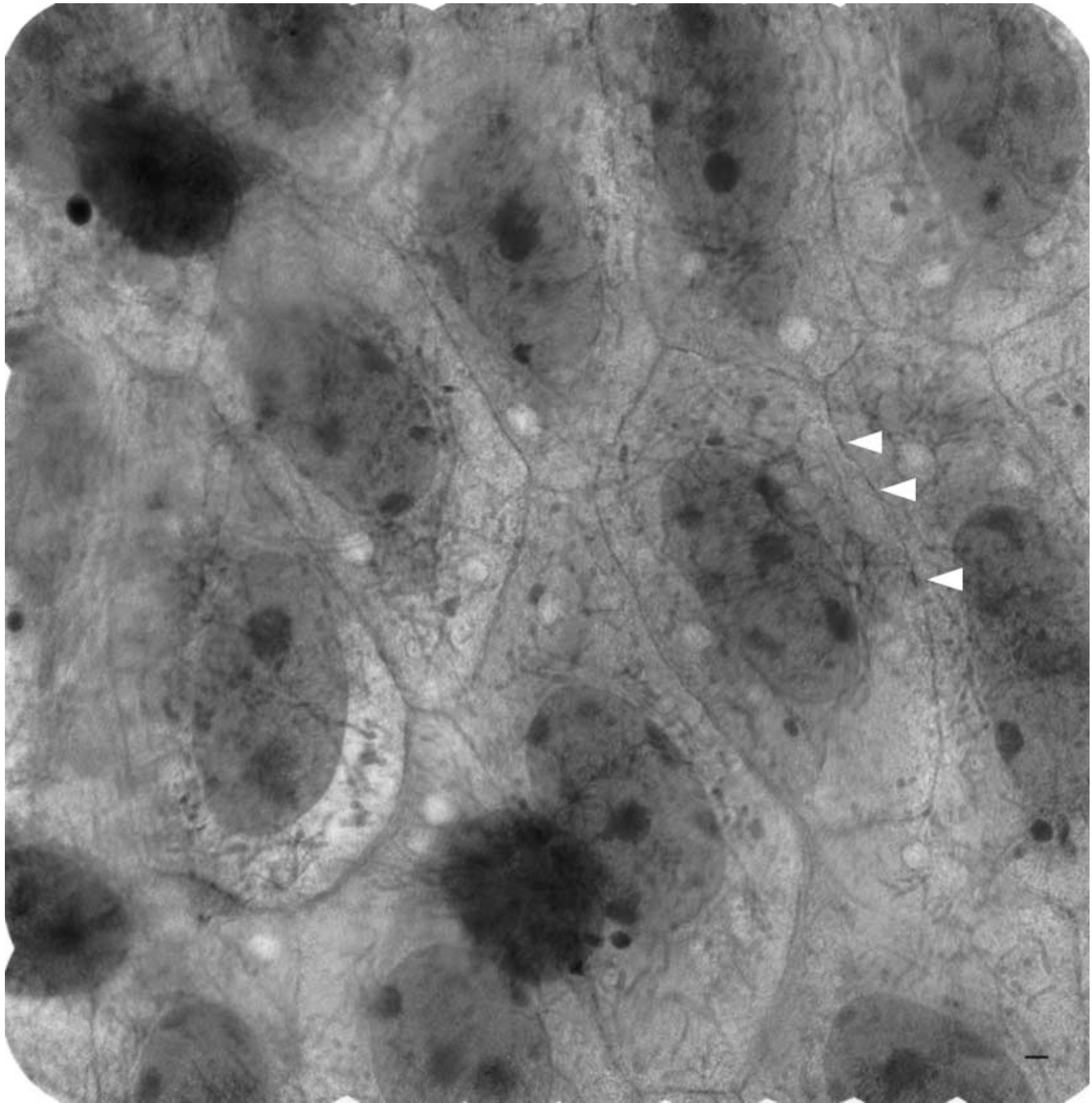


Fig. 6. Soft X-ray micrographs illustrating microtubules in two pillar cells. Scale bar, 1  $\mu\text{m}$ .



**Fig. 7.** Soft X-ray micrograph (tiled image) of the Reissner's membrane from the guinea-pig cochlea. About 15 cells can be seen in the photograph. The arrowheads indicate desmosomes. Scale bar, 1  $\mu\text{m}$ .

microscopy. This is a relatively new and potentially powerful tool for observing microstructures in biological tissues (Meyer-Ilse *et al.*, 1995; Jacobsen, 1999; Yamamoto & Shinohara, 2002). At present, the resolution of the soft X-ray microscope falls between that of a light microscope and an electron microscope. In this report we explore for the first time the use of soft X-ray microscopy for imaging sensory and supporting cells from the

hearing organ as well as the adjacent Reissner's membrane and tectorial membrane. The hair cells contain complex structures, e.g. filaments and microtubules that are vital for the function of the cell, and these carbon-dense structures should be readily visualized using soft X-ray microscopy. As the diameter of the sensory hair cells is only about 10  $\mu\text{m}$  – the maximal height of a structure that will fit the present

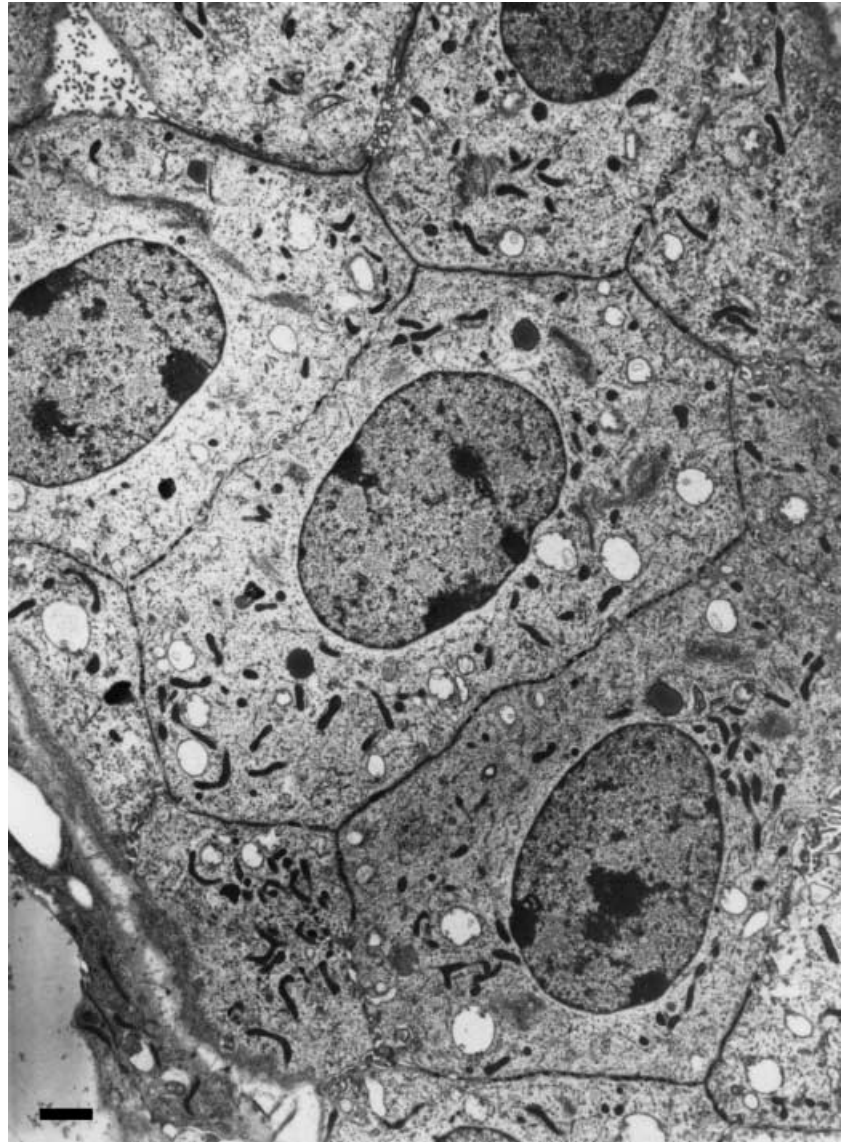


**Fig. 8.** Electron micrograph showing the Reissner's membrane (plastic embedded and sectioned along a plane parallel to its surface) at a similar orientation as in Fig. 7. Scale bar, 2  $\mu\text{m}$ .

experimental chamber at the ALS soft X-ray microscope—they are very suitable as objects for testing the performance of the soft X-ray microscope.

Soft X-ray microscopy utilizes a natural photon absorption contrast between carbon and oxygen atoms at water-window wavelengths (2.3–4.4 nm) (Kirz *et al.*, 1995; Jacobsen, 1999). This makes it a particularly attractive method for studying biological samples in their natural hydrated state, because they consist of carbon-rich structures surrounded by oxygen-rich water. Consequently, even thin protein structures will strongly absorb photons, whereas water remains relatively transparent up to a thickness of 10  $\mu\text{m}$ . Contrary to traditional microscopy, there are no contrast or labelling substances that readily can be used. However, immunogold labelling has previously been used to localize specific proteins (Meyer-Ilse *et al.*, 2001).

The images of the sensory hair cells from the inner ear illustrate an important limitation of the soft X-ray microscope. Although the cells are well within the 10- $\mu\text{m}$  constraint of the wet cell, there are clearly structures that are too thick or carbon-dense to visualize, e.g. the cuticular plate (cf. Fig. 2) and nucleus (cf. Fig. 3). On the other hand, thinner structures such as membranes, stereocilia (cf. Fig. 2), cytoplasmic filaments and microtubules (cf. Figs 3 and 5) are readily imaged. It has previously been shown that soft X-ray microscopy is useful for visualizing fine fibrillar structures at cell surfaces, and produces more reliable results than electron microscopy (Yamamoto & Shinohara, 2002).

If resolution were the only issue, soft X-ray microscopy would not be such an interesting alternative to electron microscopy. The image quality and resolution offered by transmission electron microscopy are obviously superior to that of

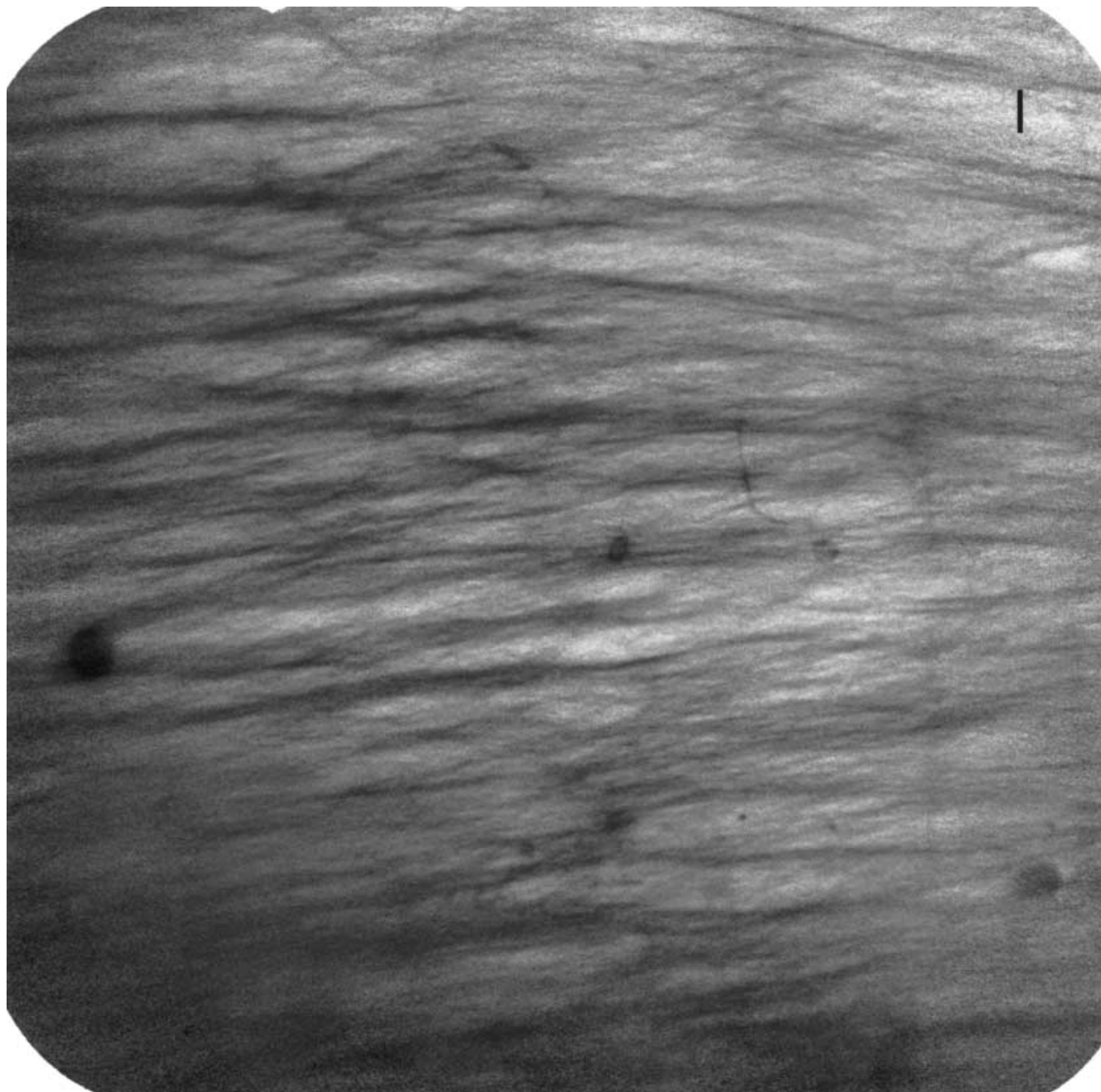


**Fig. 9.** Soft X-ray micrograph (tiled image) illustrating the tectorial membrane from the guinea-pig cochlea clearly showing the transverse collagen fibre bundles and fibres. Scale bar, 1  $\mu\text{m}$ .

the X-ray microscope. However, the fundamental advantage of the X-ray microscope is that it allows visualization of cells immersed in a buffer, i.e. non-dehydrated and non-embedded tissue. This is an important step to minimize artefacts, e.g. tissue shrinkage, prior to visualization. By imaging these structures with the cell in its natural hydrated state and with higher resolution than is possible using visible light microscopy, it should be possible to gain more knowledge about the

structures involved in cellular function. Moreover, eliminating many of the time-consuming steps, such as dehydration, embedding and sectioning, associated with electron microscopy would drastically increase the experimental throughput. The time-period from dissecting the tissue until viewing the print easily exceeds 1 week (9 days in the present study). By contrast, the time required for placing the tissue in the test chamber of the X-ray microscope and obtaining an image was

approximately 15 min. The turnaround time was reduced by a factor of nearly 300. It is obvious that such a large reduction in the time needed to examine a tissue specimen has important consequences for this application.

Image quality and resolution are limited by the fact that the high energy of the X-rays damages protein structures and causes the tissue to shrink (Schneider, 1998). However, it should also be kept in mind that conventional electron microscopy is associated with significant tissue changes due to radiation damage and the vacuum requirement. This shrinkage can be reduced by converting the tissue to a more radiation-resistant form, i.e. by fixing the tissue.

In the present study, it was necessary to use chemical fixation (glutaraldehyde) to stabilize the tissue prior to X-ray exposure. An attractive alternative would be to use cryofixation because it would inhibit morphological changes and structural deterioration resulting from radiation damage. The procedure would also prevent movement of cells that are not fixed to the silicon nitride membrane surface. The soft X-ray group in Göttingen, Germany, started work on cryo transmission X-ray microscopy and they have shown that vitrified samples are stable up to a dosage of  $10^{10}$  Gy (Schneider, 1998), i.e. the structural radiation damage is less than can be detected at the resolution used. Normally, a single exposure gives a dose of approximately  $10^7$  Gy to the sample. Cryofixation has previously been used with outstanding results at the ALS soft X-ray microscope (Meyer-Ilse *et al.*, 2001), but the feature was unfortunately not available during this study.

Soft X-ray microscopy is very much at its beginning and further technical improvements are required before it can be used more generally to complement electron microscopy in experimental research. Unfortunately, one of the limitations to a wider use of soft X-ray microscopy is the necessity to use a strong beam of X-rays, which means that experiments must be performed at synchrotron radiation facilities such as the ALS. To facilitate experimental investigations in environments more suited for biomedical experiments, it would be useful to develop instruments using table-top soft X-ray sources that can still provide high-resolution imaging (Johansson *et al.*, 2002). For example, it was previously shown that outer hair cell shortening was correlated with a more undulated cell membrane (Ulfendahl & Slepecky, 1988). This observation, based on a very laborious electron microscope analysis of individual fixed, dehydrated, embedded and sectioned cells, could have been much more straightforward using high-resolution soft X-ray microscopy. For future studies on the structural and subcellular changes related to outer hair cell motility, soft X-ray microscopy could be of great value.

### Acknowledgements

We wish to thank Angelic Pearson, Erik Anderson, Bill Bates, Weilun Chao, Kathleen Fuller, Randy Deguzman and Gerd Schneider for valuable help and support during the experi-

ments. G.A.J. also wishes to thank Hans Hertz and David Attwood for providing him with the opportunity to visit the Center for X-ray Optics. This work was supported by grants from the Swedish Research Council, the Foundation Tysta Skolan, the Emil Capita Foundation, and the Swedish Foundation for International Cooperation in Research and High Education (STINT).

### References

- Anderson, E.H., Olynick, D.L., Harteneck, B., Veklerov, E., Denbeaux, G., Chao, W., Lucero, A., Johnson, L. & Attwood, D. Jr (2000) Nanofabrication and diffractive optics for high-resolution X-ray applications. *J. Vac. Sci. Technol.* **18**, 2970–2975.
- Attwood, D. (1999) *Soft X-rays and Extreme Ultraviolet Radiation: Principles and Applications*. Cambridge University Press, Cambridge.
- Denbeaux, G., Anderson, E., Chao, W., Eimüller, T., Johnson, L., Köhler, M., Larabell, C., Legros, M., Fischer, P., Pearson, A., Schütz, G., Yager, D. & Attwood, D. (2001) Soft X-ray microscopy to 25 nm with applications to biology and magnetic materials. *Nucl. Instr. Meth. A*, **467–468**, 841–844.
- Djabali, K. (1999) Cytoskeletal proteins connecting intermediate filaments to cytoplasmic and nuclear periphery. *Histol. Histopathol.* **14**, 510–509.
- Jacobsen, C. (1999) Soft X-ray microscopy. *Trends Cell Biol.* **9**, 44–47.
- Johansson, G.A., Holmberg, A., Hertz, H.M. & Berglund, M. (2002) Design and performance of a laser-plasma based compact soft X-ray microscope. *Rev. Sci. Instrum.* **73**, 1193–1197.
- Kikuchi, T., Takasaka, T., Tonosaki, A., Katori, Y. & Shinkawa, H. (1991) Microtubules of guinea pig epithelial cells. *Acta Otolaryngol. (Stockholm)*, **111**, 286–290.
- Kirz, J., Jacobsen, C. & Howells, M. (1995) Soft X-ray microscopes and their biological applications. *Q. Rev. Biophys.* **28**, 33–130.
- Kronester-Frei, A. (1978) Ultrastructure of the different zones of the tectorial membrane. *Cell Tiss. Res.* **193**, 11–23.
- Loo, B.W., Jr, Meyer-Ilse, W. & Rothman, S.S. (2000) Automatic image acquisition, calibration and montage assembly for biological X-ray microscopy. *J. Microsc.* **197**, 185–201.
- Meyer-Ilse, W., Denbeaux, G., Johnson, L.E., Bates, W., Lucero, A. & Anderson, E.H. (1999) The high resolution X-ray microscope, XM-1. *X-ray microscopy VI. XRM99* (ed. by W. Meyer-Ilse, T. Warwick and D. Attwood), pp. 129–134. American Institute of Physics, Melville, NY.
- Meyer-Ilse, W., Hamamoto, D., Nair, A., Lelièvre, S.A., Denbeaux, G., Johnson, L., Pearson, A.L., Yager, D., Legros, M.A. & Larabell, C.A. (2001) High resolution protein localization using soft X-ray microscopy. *J. Microsc.* **201**, 395–403.
- Meyer-Ilse, W., Medeck, H., Jochum, L., Anderson, E., Attwood, D., Magowan, C., Balhorn, R., Moronne, M., Rudolph, D. & Schmahl, G. (1995) New high-resolution zone-plate microscope at beamline 6.1 of the ALS. *Synchrotron Radiation News*, **8**, 29–33.
- Schmahl, G., Rudolph, D., Niemann, B., Guttman, P., Thieme, J., Schneider, G., David, C., Diehl, M. & Wilhein, T. (1993) X-ray microscopy studies. *Optik*, **93**, 95–102.
- Schneider, G. (1998) Cryo X-ray microscopy with high spatial resolution in amplitude and phase contrast. *Ultramicroscopy*, **75**, 85–104.
- Slepecky, N.B. (1996) Structure of the mammalian cochlea. *The Cochlea* (ed. by P. Dallos, A. N. Popper and R. R. Fay), pp. 44–129. Springer-Verlag, New York.

- Slepecky, N. & Ulfendahl, M. (1992) Actin-binding and microtubule-associated proteins in the organ of Corti. *Hearing Res.* **57**, 201–215.
- Steyger, P.S., Furness, D.N., Hackney, C.M. & Richardson, G.P. (1989) Tubulin and microtubules in cochlear hair cells: comparative immunocytochemistry and ultrastructure. *Hearing Res.* **42**, 1–16.
- Thorne, P.R., Carlisle, L., Zajic, G., Schacht, J. & Altschuler, R.A. (1987) Differences in the distribution of F-actin in outer hair cells along the organ of Corti. *Hearing Res.* **30**, 253–265.
- Tsuprun, V. & Santi, P. (1996) Crystalline arrays of proteoglycan and collagen in the tectorial membrane. *Matrix Biology*, **15**, 31–38.
- Tsuprun, V. & Santi, P. (1997) Ultrastructural organization of proteoglycans and fibrillar matrix of the tectorial membrane. *Hearing Res.* **110**, 107–118.
- Ulfendahl, M. & Slepecky, N. (1988) Ultrastructural correlates of inner ear sensory cell shortening. *J. Submicrosc. Cytol. Pathol.* **20**, 47–51.
- Yamamoto, Y. & Shinohara, K. (2002) Application of X-ray microscopy in analysis of living hydrated cells. *Anat. Rec.* **269**, 217–223.
- Zenner, H. (1986) Motile responses in outer hair cells. *Hearing Res.* **22**, 83–90.